# Supplementary Information

## Glutathione-Responsive Self-Assembled Magnetic Gold Nanowreath for Enhanced Tumor Imaging and Imaging-Guided Photothermal Therapy

Yijing Liu,[†] Zhen Yang,[†] Xiaolin Huang,[†,‖] Guocan Yu,[†] Sheng Wang,[†] Zijian Zhou,[†] Zheyu Shen,[*,†,§] Wenpei Fan,[†] Yi Liu,[‡#] Matthew Davisson,[⊥] Heather Kalish,[⊥] Gang Niu,[†] Zhihong Nie,[*,‡] and Xiaoyuan Chen[*,†]

[†]Laboratory of Molecular Imaging and Nanomedicine, National Institute of Biomedical Imaging and Bioengineering, National Institutes of Health, Bethesda, MD 20892, USA

[‡]Department of Chemistry and Biochemistry, University of Maryland, College Park, Maryland, 20742, USA

[§]CAS Key Laboratory of Magnetic Materials and Devices, Key Laboratory of Additive Manufacturing Materials of Zhejiang Province, and Division of Functional Materials and Nanodevices, Ningbo Institute of Materials Technology and Engineering, Chinese Academy

of Sciences, 1219 Zhongguan West Road, Ningbo, Zhejiang 315201, China

[‖]State Key Laboratory of Food Science and Technology, Nanchang University, Nanchang 330047, P. R. China

[⊥]Trans-NIH Shared Resource on Biomedical Engineering and Physical Science. Institute of Biomedical Imaging and Bioengineering, National Institutes of Health, Bethesda, MD 20892, USA

[#]State Key Laboratory of Supramolecular Structure and Materials, College of Chemistry, Jilin University, Changchun 130012, P. R. China

**Corresponding Authors**

E-mail: shawn.chen@nih.gov (X.C.); znie@umd.edu (Z.N.); shenzheyu@nimte.ac.cn (Z.S.)

**Supplementary Figures**

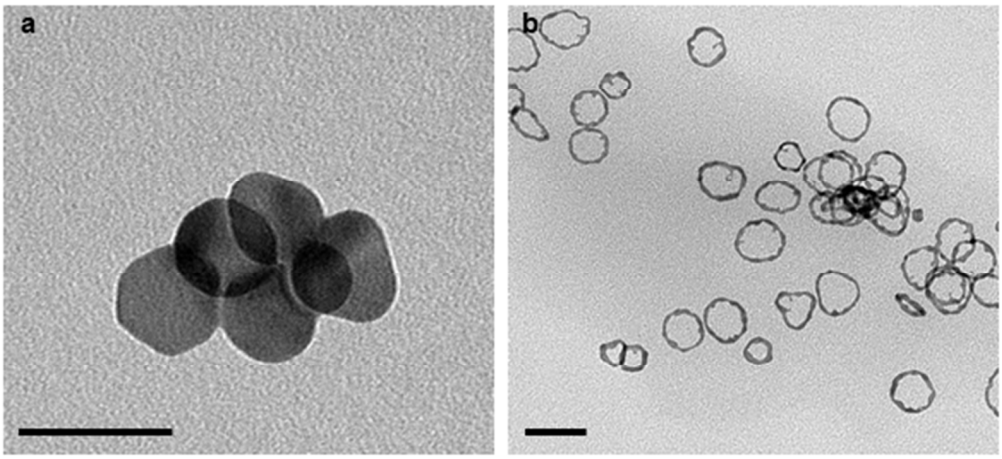


**Figure S1. TEM images of (a) silver (Ag) nanoplate templates and (b) initial gold (Au) nanoring templates.** Scale bars: 50 nm.

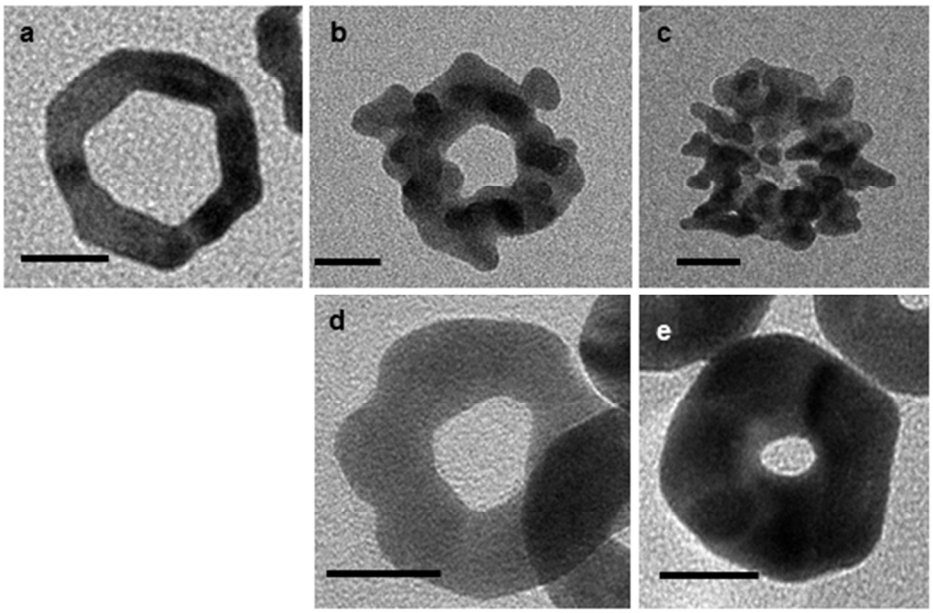


**Figure S2. Representative TEM images of the Au nanoring seeds and other Au nanostructures made from Au nanoring seeds.** (a) TEM image of Au nanoring seed. (b,c) TEM images of Au nanowreath (AuNW) with (b) short branches and (c) long branches by controlling the ratio of hydrogen tetrachloroaurate(III) trihydrate ($HAuCl4 \cdot 3H_2O$) to Au nanoring seeds. (d,e) TEM images of thick Au nanoring with smooth surface and relatively (d) thinner or (e) thicker thickness by controlling the ratio of $HAuCl_4 \cdot 3H_2O$ to Au nanoring seeds. Scale bars: 20 nm

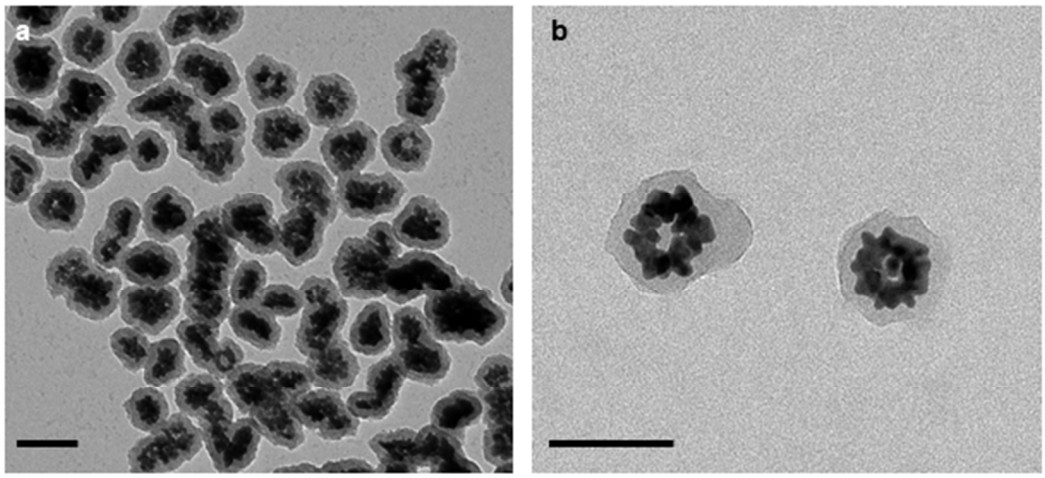


**Figure S3. Representative TEM images of AuNW@Silica (AuNW@$SiO_2$) nanoparticles.** Scale bars: 100 nm

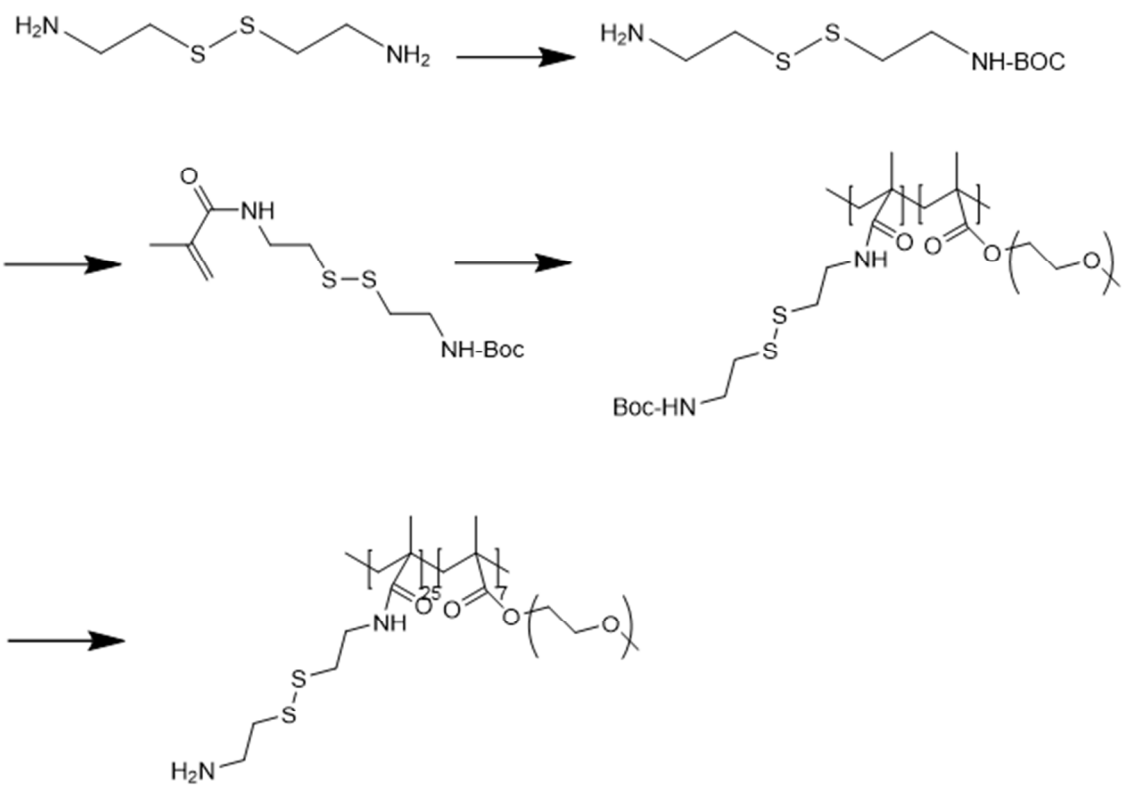


**Figure S4. Synthesis procedure for polycystamine-co-polyoligo(ethylene glycol) methyl ether methacrylate.**

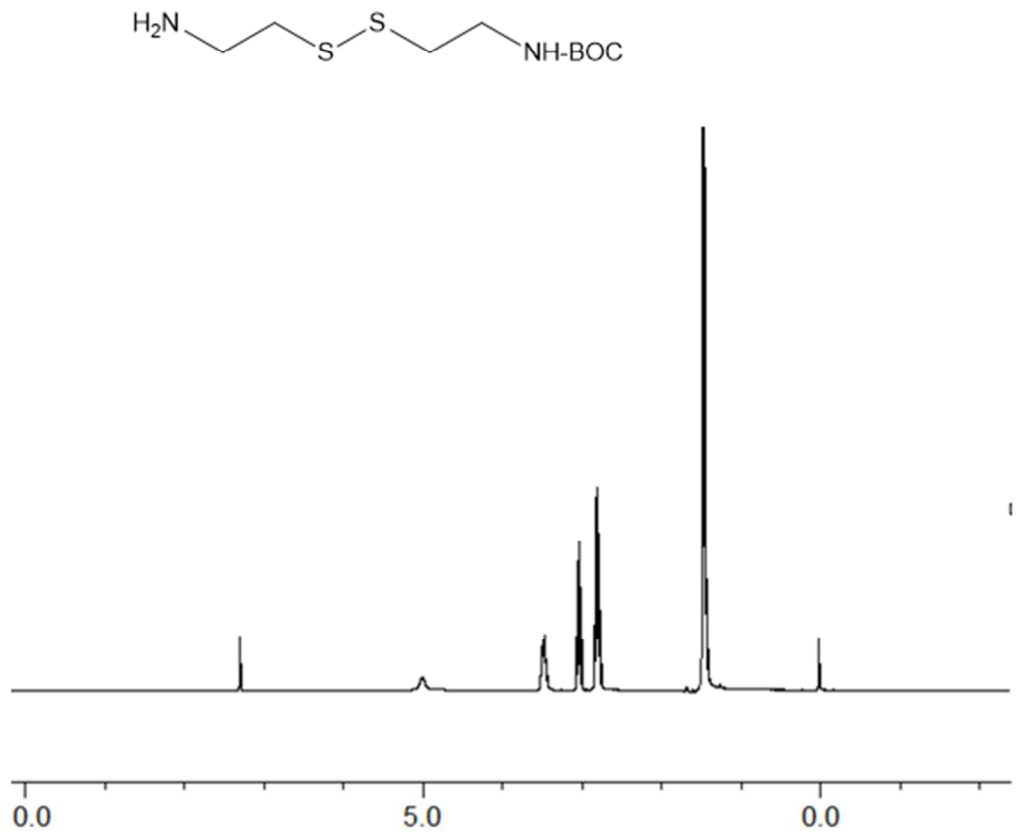


**Figure S5. $^{1}$H NMR spectra of mono–Boc–cystamine, $CDCl_3$ as a solvent**

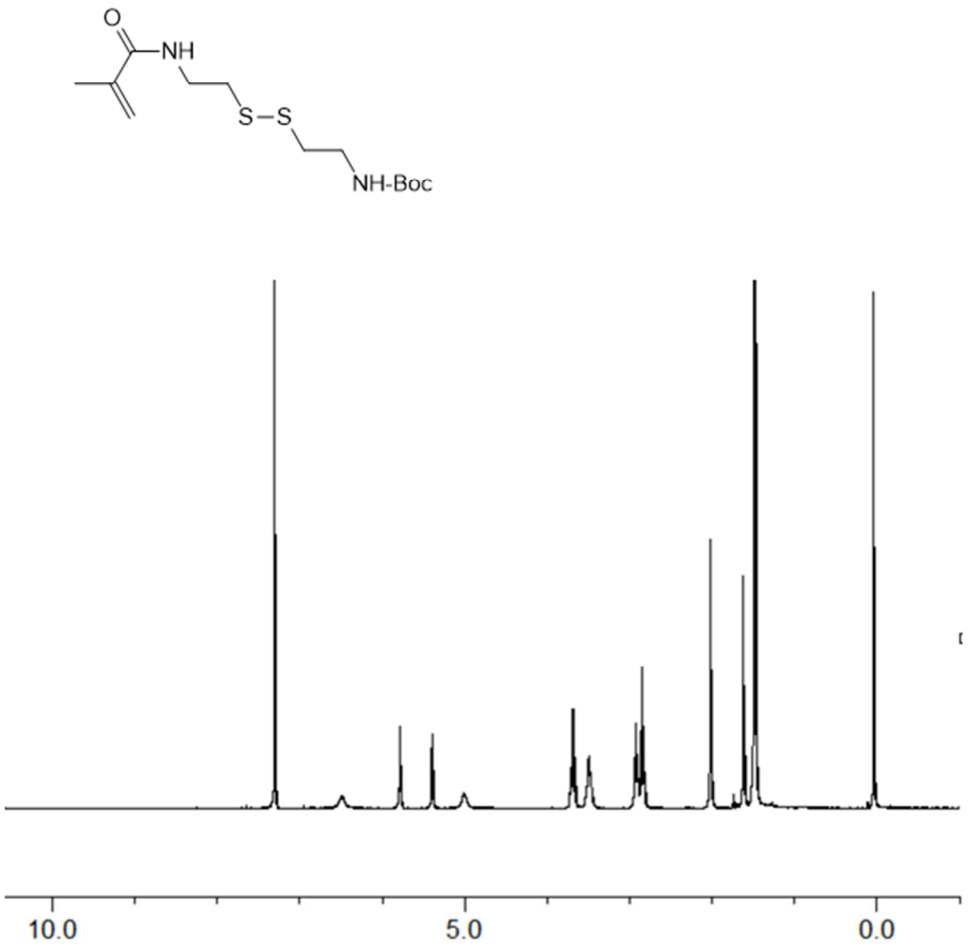


**Figure S6. $^{1}$H NMR spectra of mono-Boc-cystamine methacrylamide, $CDCl_3$ as a solvent**

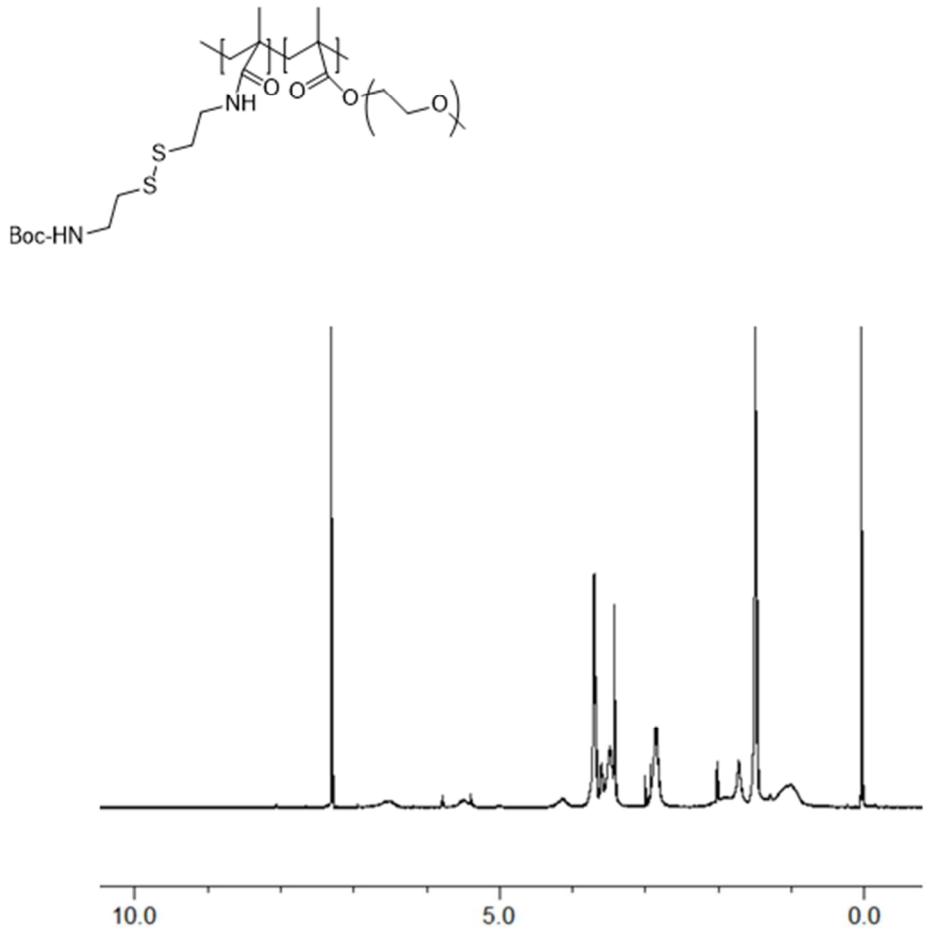


**Figure S7. $^{1}$H NMR spectra of poly boc-cystamine-co-polyoligo(ethylene glycol) methyl ether methacrylate, $CDCl_3$ as a solvent**

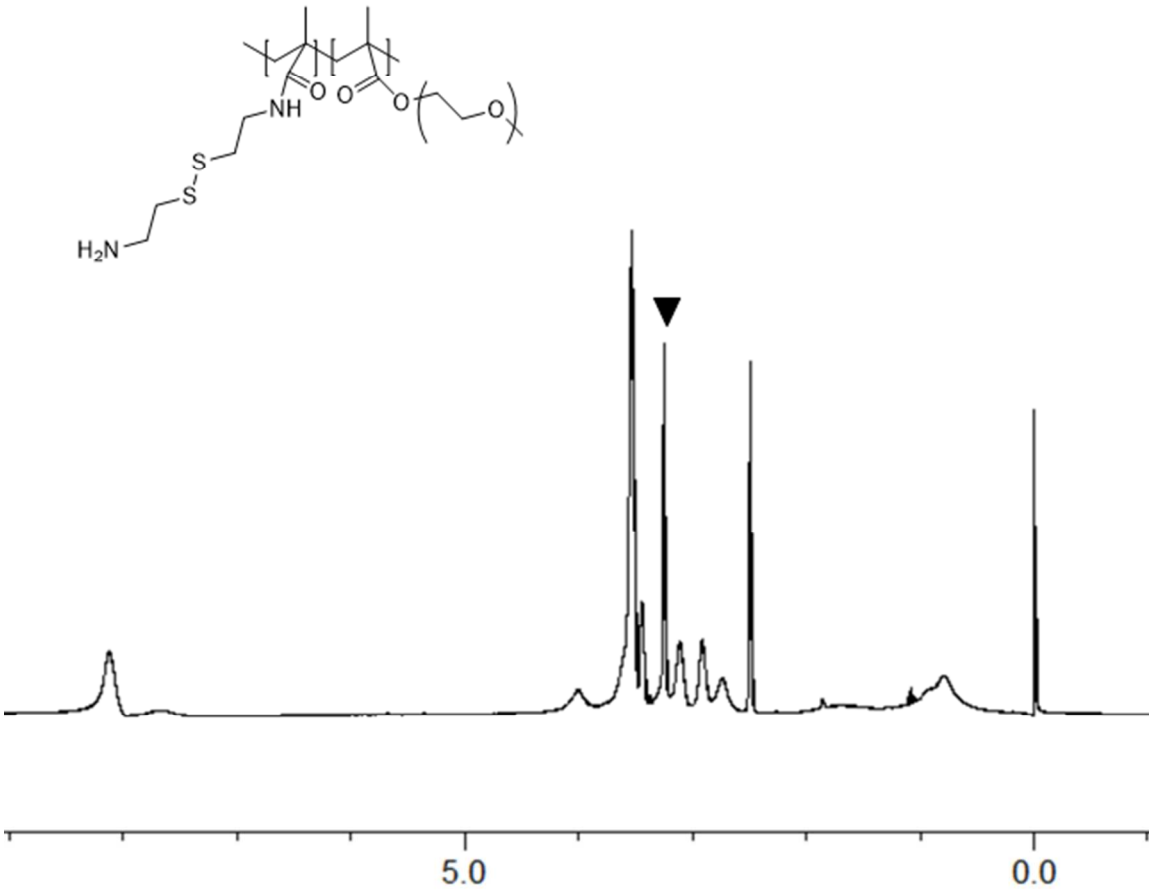


**Figure S8.** $^{1}$**H NMR spectra of poly cystamine-co-polyoligo(ethylene glycol) methyl ether methacrylate, DMSO-d$_6$ as a solvent. ▼ indicates the peak of water.**

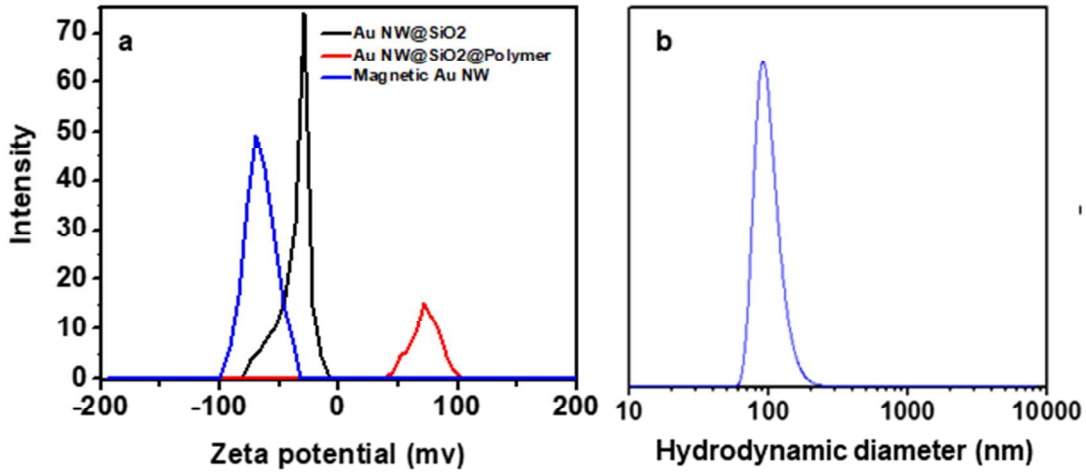


**Figure S9. The zeta-potential characterization and dynamic light scattering characterization of magnetic AuNWs.** (a) The surface charge conversion process during the layer-by-layer self-assembly and (b) the measurement of the hydrodynamic diameter of magnetic AuNWs

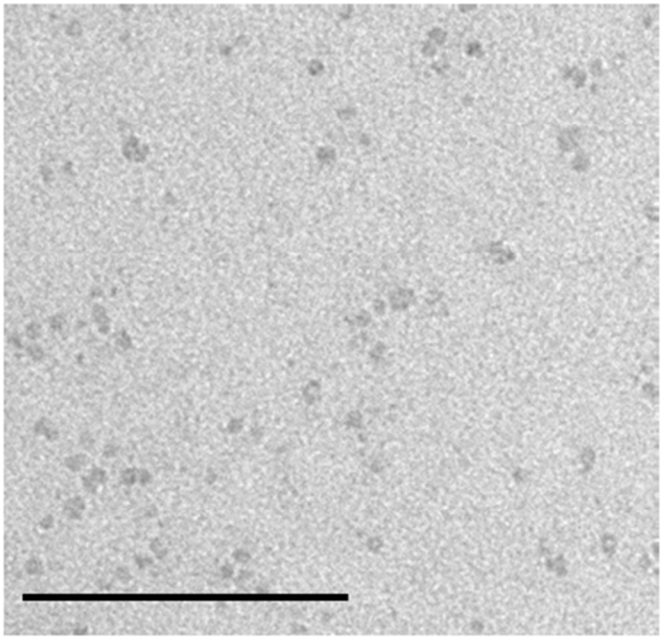

**Figure S10. Representative TEM image of the exceedingly small magnetic iron oxide nanoparticles (ES-MIONs).** Scale bar: 100 nm.

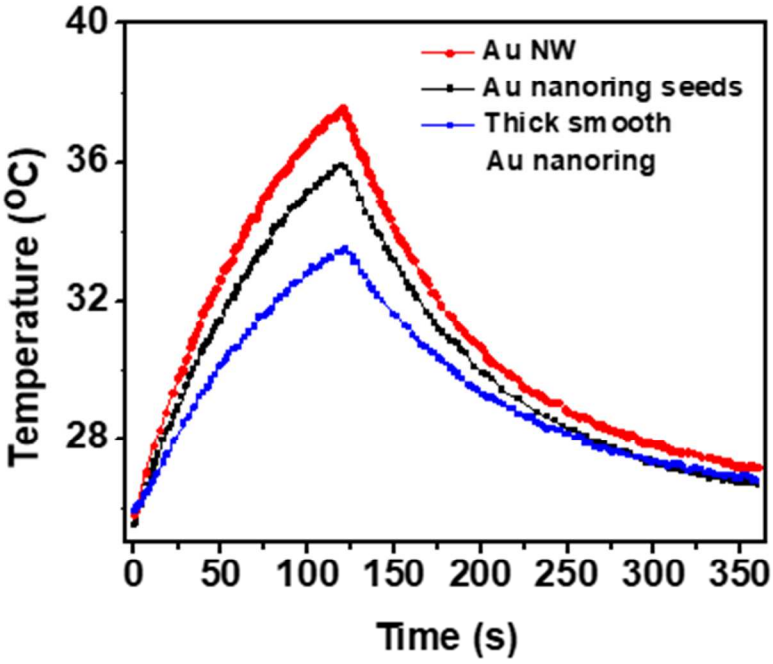


**Figure S11. Photothermal characterization of AuNWs, Au nanoring seeds, and thick Au nanorings with smooth surface.** The nanostructures used in this experiment are corresponding to the nanostructures shown in Figure S2c, Figure S2a, and Figure S2e, respectively. The aqueous dispersion of these nanostructures was irradiated by an 808 nm laser at 0.25 W/cm$^2$ for 2 min.

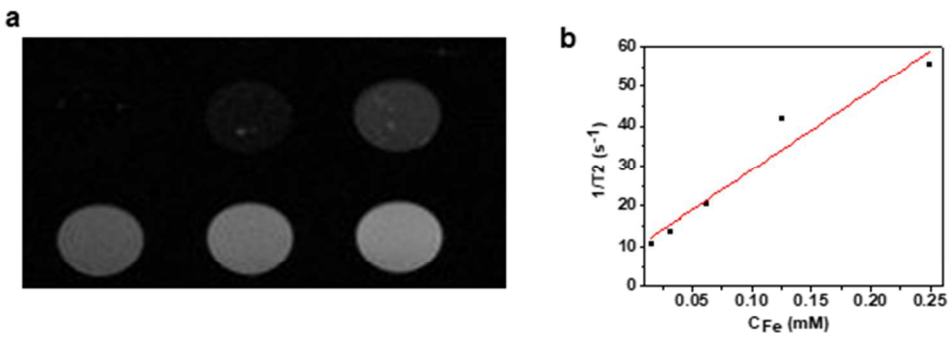


**Figure S12 $T_2$ MRI characterizations of assembled magnetic AuNWs.** (a) $T_2$-weighted images and (b) plot of $r_2$ value of assembled magnetic AuNWs (y = 198.577 x + 9.156). The concentrations in $T_2$-weighted images from left to right are 0.5, 0.25, 0.125 (first row), 0.0625, 0.03125, and 0.01563 mM (second row).

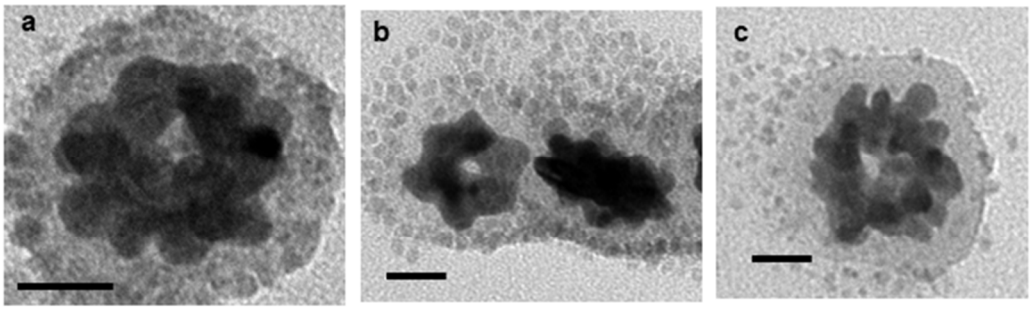


**Figure S13. Representative TEM images of the disassembly of ES-MIONs from magnetic AuNW in 10 mM Glutathione (GSH).** The TEM images were taken (a) before incubation with GSH and at (b) 0.5 h and (c) 2 h incubation with 10 mM GSH solution.

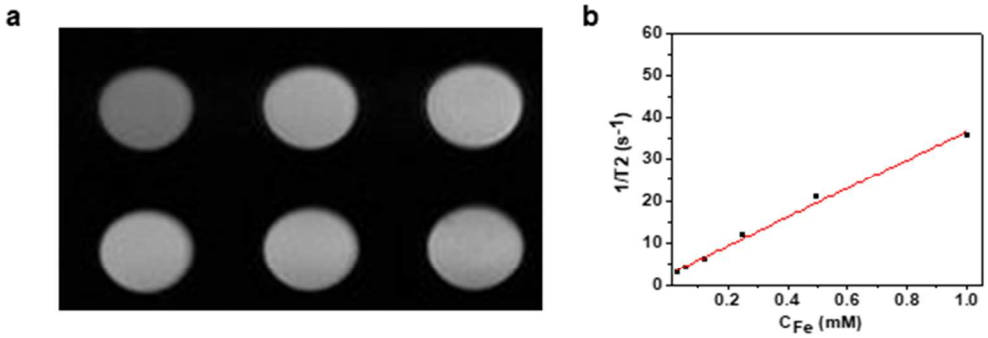


**Figure S14. $T_2$ MRI characterizations of disassembled magnetic AuNWs.** (a) $T_2$-weighted images and (b) plot of $r_2$ value of disassembled magnetic AuNWs (y = 33.9 x + 2.53). The concentrations in $T_2$-weighted images from left to right are 1, 0.5, 0.25 (first row), 0.125, 0.0625, and 0.03125 mM (second row).

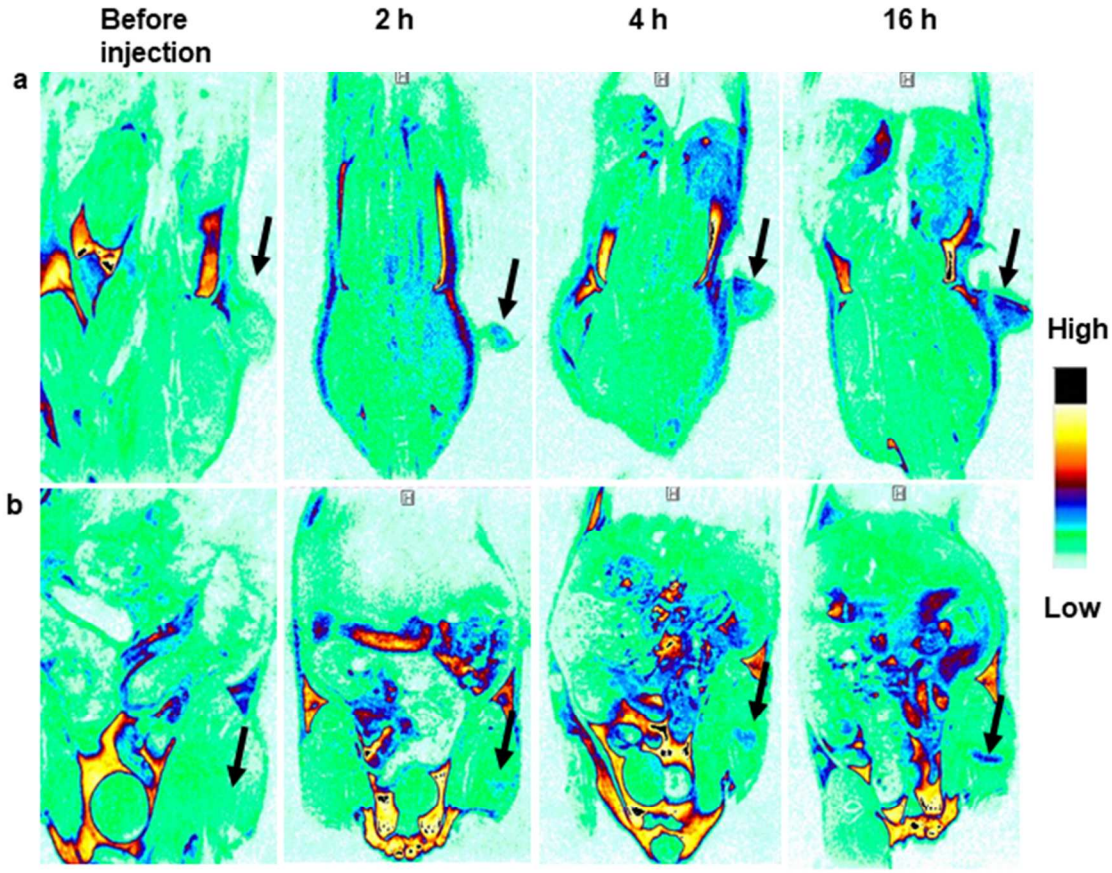

**Figure S15. Comparison of $T_1$-weighted MR imaging of magnetic AuNWs after their local injection in (a) tumor and (b) muscle.** The images in each row from left to right were taken before injection of magnetic AuNWs, and at 2, 4, and 16 h post-injection. The black arrows indicate the signals from injection sites.

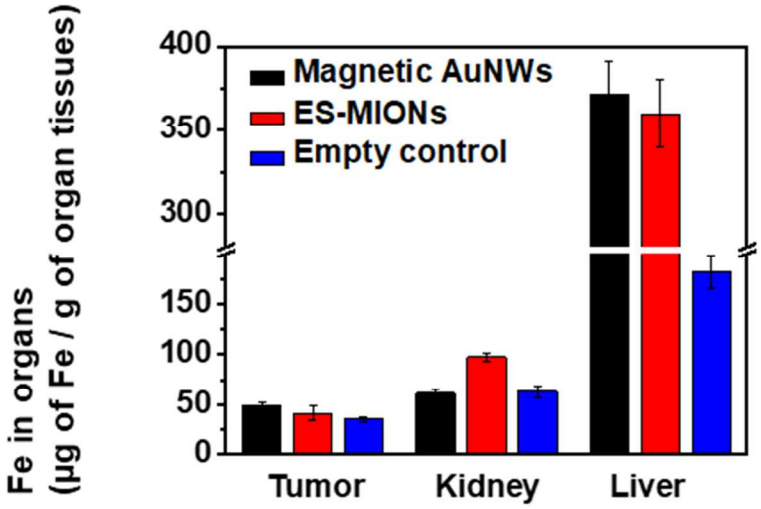


**Figure S16. The concentrations of Fe in tumors, kidneys, and livers after intravenous injection of magnetic AuNWs, ES-MIONs, and PBS.** The tumors and other organs were collected, weighted, and digested at 24 h post-injection and concentrations of Fe were analyzed by ICP. The Fe doses of both magnetic AuNWs and ES-MIONs for injection were set at 15 mg/kg.

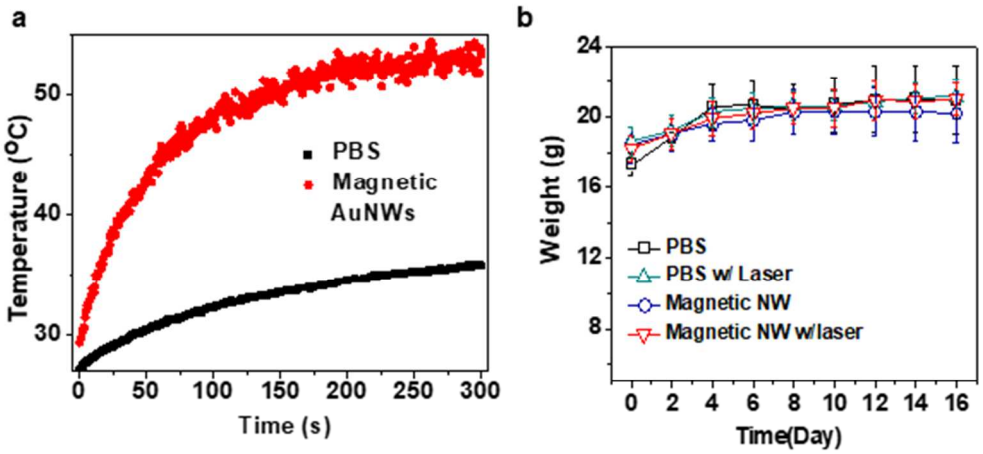


**Figure S17. Photothermal therapy with magnetic AuNWs.** (a) The corresponding temperature increasing curves of tumor areas after injection of magnetic AuNWs and PBS upon laser irradiation for 5 min (0.75 W/cm$^2$) and (b) body weight curves of treatment group and all other control groups.

**Supplementary Methods**

**Characterizations.** The TEM images of magnetic AuNWs and other nanostructures were characterized by a Tecnai Spirit TEM (FEI). SEM images were obtained *via* a Hitachi SU-70 Schottky FEG-SEM. UV-Vis absorption was measured by a Genesys 10S UV-vis spectrophotometer. HAADF image and EDS line scan measurement were obtained from a JEM 2100 FEG TEM. The hydrodynamic diameters of AuNPs were measured by a Zetasizer Nano series. The concentrations of Au and Fe of NPs were characterized by an ICP-OES. The fluorescence images of cells were taken by an Olympus IX81 fluorescence microscope. PA/US imaging was performed on a Visual Sonics Vevo LAZR system (VisualSonics Inc. New York, NY). The MRI characterizations were conducted by a Bruker MRI scanner (7.0 T, B-C 70/16, Bruker, US).

**Evaluation of the toxicity and photothermal induced cell killing of magnetic AuNWs.** U87MG cells were seeded in 96-well plates containing Minimum Essential Medium (MEM) with 10 % of fetal bovine serum (FBS) and 1% penicillin and streptomycin at the density of $5 \times 10^3$ cells/well for 24 h before different amounts of magnetic AuNWs were added. For *in vitro* cytotoxicity study, the MEM in 96-well plates was removed after 24 h incubation with NPs, and a 100 μL MEM with 1 mg/mL MTT was added into each well and the plates were incubated at 37 °C for another 4 h. Then, the MTT was taken out and the 96-well plates were refilled with 100 μL DMSO. The absorbance at 570 nm from each well was recorded and was compared to the signal from cell-seeded wells free of magnetic AuNWs. For photothermal induced cell killing experiment, after incubation of cells with NPs for 24 h, the NPs containing MEM was replaced by NP free MEM. Then each well was irradiated by an 808 nm laser at power density of 0.75 W/cm$^2$ for ten min and the same MTT procedure was used to evaluate the viability of cells. To monitor the

photothermal treatment effect on cells, fluorescence images of cells stained by calcein, AM and ethidium bromide were acquired. Specifically, $2 \times 10^5$ cells were seeded in each well of 6-well plates overnight. Then, magnetic AuNWs were added into each well for 24 h before an 808 nm laser was irradiated at cells. The live and dead cells were then co-stained by calcein, AM and ethidium bromide in PBS for 30 min before the fluorescence images were taken.

**Animal Models.** All animal experiments were performed under the National Institutes of Health Animal Care and Use Committee (NIHACUC) approved protocol. $3 \times 10^6$ U87MG cells were injected at right hind leg to induce the growth of subcutaneous tumors.

***In vivo*** **MRI characterizations**. The anaesthetized nude mice were placed in an MRI coil for animals with body temperature maintained at 37 $^0$C and respiration monitored by a sensor. For local injection, same amount magnetic AuNWs were injected into tumor and muscle, respectivley. The $T_1$-weight images of tumor and muscle were acquired before the injection of magnetic AuNWs and at 2, 4, and 16 h post-injection. For intravenous injection, the $T_1$-weight images of tumor were acquired before the injection of magnetic AuNWs and at 2, 12, 24, and 48 h post-injection. As comparison, $T_1$-weight images of tumor by Magneveist and individual ES-MIONs were also acquired at different time points post-injection. The amount of injected contrast agents was set at 5.0 mg / kg for all. Multi-slice multi-echo sequence was employed to acquire images using parameters as follows: repetition time (TR) = 400 ms, echo time (TE) = 8 ms, flip angle = $180^o$ , matrix size = $256 \times 256$

The acquired MR images were analyzed by Image J to obtain the signal intensity. The signal-to-noise ratio (SNR) and signal enhancement were calculated according to the following equations

SNR = SImean / SDnoise,

In which SImean refers to the average signal intensity of interest area (tumor) obtained from Image J analysis, and SDnoise represents the standard deviation of the signal intensity of different background locations.

Signal enhancement = SNRpost / SNRpre.

In which, SNRpost and SNRpre refer to the calculated SNR after and before the injection of the MRI contrast agents, respectively.

**Evaluation of photothermal treatment.** The tumor-bearing mice were divided into 4 groups with 5 mice in each group. These groups include, mice with injection of PBS, mice with injection of magnetic AuNWs without laser irradiation, mice with laser irradiation without injection of NPs. When the tumor volume reached 100 $mm^3$, PBS or magnetic AuNWs were intravenously injected accordingly. At 24 h after injection, an 808 nm laser was irradiated at tumor for the laser irradiation group at 0.75 $W/cm^2$ for 5 min. The tumor growth and weight of mice were recorded every two days.